

Molecular Characteristics of Catechol Estrogen Quinones in Reactions with Deoxyribonucleosides

Douglas E. Stack,[†] Jaeman Byun,[‡] Michael L. Gross,[‡] Eleanor G. Rogan,[†] and Ercole L. Cavalieri^{*,†}

Eppley Institute for Research in Cancer and Allied Diseases, University of Nebraska Medical Center, 600 South 42nd Street, Omaha, Nebraska 68198-6805, and Department of Chemistry, Washington University, One Brookings Drive, St. Louis, Missouri 63130-4899

Received January 2, 1996[®]

Estrogens can have two roles in the induction of cancer: stimulating proliferation of cells by receptor-mediated processes, and generating electrophilic species that can covalently bind to DNA. The latter role is thought to proceed through catechol estrogen metabolites, which can be oxidized to *o*-quinones that bind to DNA. Four estrogen–deoxyribonucleoside adducts were synthesized by reaction of estrone 3,4-quinone (E₁-3,4-Q), 17 β -estradiol 3,4-quinone (E₂-3,4-Q), or estrone 2,3-quinone (E₁-2,3-Q) with deoxyguanosine (dG) or deoxyadenosine (dA) in CH₃CO₂H/H₂O (1:1). Reaction of E₁-3,4-Q or E₂-3,4-Q with dG produced specifically 7-[4-hydroxyestron-1(α,β)-yl]guanine (4-OHE₁-1(α,β)-N7Gua) or 7-[4-hydroxyestradiol-1(α,β)-yl]guanine (4-OHE₂-1(α,β)-N7Gua), respectively, in 40% yield, with loss of deoxyribose. These two quinones did not react with dA, deoxycytidine, or thymidine. When E₁-2,3-Q was reacted with dG or dA, N²-(2-hydroxyestron-6-yl)deoxyguanosine (2-OHE₁-6-N²dG, 10% yield) and N⁶-(2-hydroxyestron-6-yl)deoxyadenosine (2-OHE₁-6-N⁶dA, 80% yield), respectively, were formed. These adducts provide insight into the type of DNA damage that can be caused by *o*-quinones of the catechol estrogens. The estrogen 3,4-quinones are expected to produce depurinating guanine adducts that are lost from DNA, generating apurinic sites, whereas the 2,3-quinones would form stable adducts that remain in DNA, unless repaired. The adducts reported here will be used as references in studies to elucidate the structure of estrogen adducts in biological systems.

Introduction

The role of estrogens in the induction of cancer has generally been related to stimulation of proliferation by receptor-mediated processes (1). Estrogens can also play another important role by generating electrophilic species that can covalently bind to DNA to initiate cancer (2, 3). The estrogens 17 β -estradiol (E₂)¹ and estrone (E₁), which are continuously interconverted by 17 β -oxidoreductase, are generally metabolized via two major pathways: hydroxylation at the 16 α -position and at the 2- or 4-position (4, 5). The latter pathway produces catechol estrogens (CE; Scheme 1).

In mammalian cells, CE are typically conjugated by catechol *O*-methyltransferases (COMT) to give their

monomethoxy derivatives (Scheme 1). These enzymes are protective, because only nonmethylated CE can be oxidized to their quinones (CE-Q) by peroxidases and cytochrome P450 (3, 6–9). It is hypothesized that CE-Q are the ultimate carcinogenic forms of estrogens, because these electrophiles can covalently bind to nucleophilic groups on DNA via a Michael addition. Furthermore, redox cycling generated by reduction of CE-Q to semiquinones and subsequent oxidation back to CE-Q can generate hydroxyl radicals that can cause additional DNA damage as proposed by Liehr et al. (8, 10, 11) and Nutter et al. (12, 13).

Several lines of evidence suggest that the 4-hydroxyCE are critical intermediates in the pathway leading to estrogen-induced cancer. Malignant renal tumors are induced in Syrian golden hamsters by treatment with E₁ or E₂ (14–16), suggesting that E₁ and E₂ can be procarcinogenic compounds. The CE 4-OHE₁ and 4-OHE₂ also induce renal tumors in hamsters, whereas the corresponding 2-OH isomers do not (17, 18). Furthermore, an estrogen 4-hydroxylase activity has been identified not only in hamster kidney (5, 19, 20) but also in other organs prone to estrogen-induced cancer, such as rat pituitary (21), mouse uterus (22), human MCF-7 breast cancer cells (23), human uterine myometrial tumors (24), and human breast cancer tissues (25).

Adducts formed by direct reaction of CE-Q with DNA have been compared to those formed after activation of

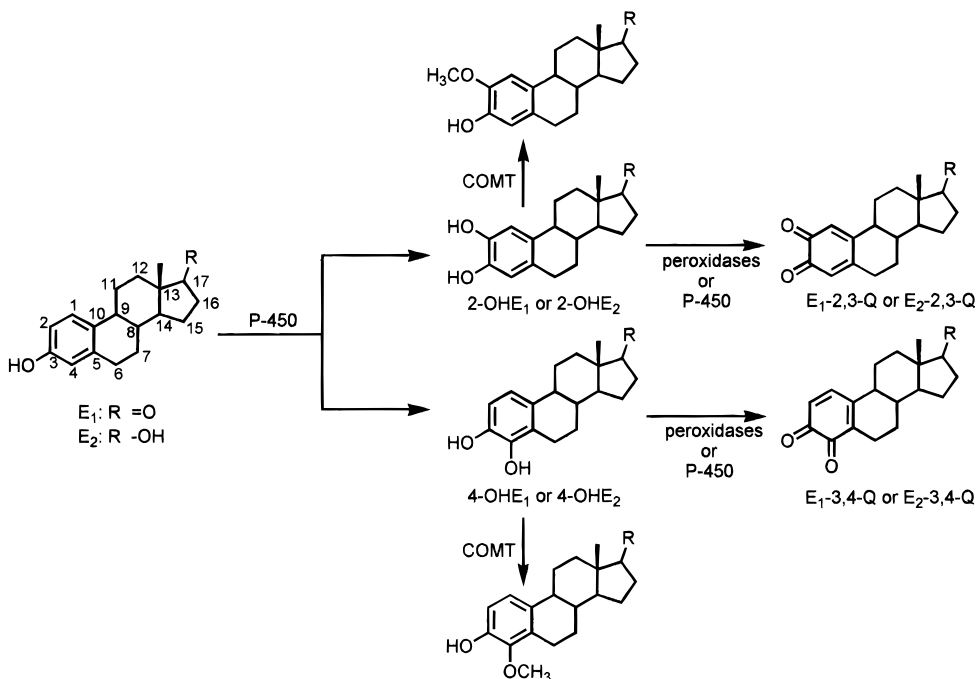
* To whom correspondence should be addressed.

[†] University of Nebraska Medical Center.

[‡] Washington University.

[®] Abstract published in *Advance ACS Abstracts*, June 15, 1996.

¹ Abbreviations: CE, catechol estrogen(s); CAD, collisionally activated decomposition; CE-Q, catechol estrogen quinone; COMT, catechol *O*-methyltransferase(s); dA, deoxyadenosine; dG, deoxyguanosine; DMF, dimethylformamide; E₁, estrone; E₂, 17 β -estradiol; E₁(E₂)-2,3-Q; estrone (estradiol) 2,3-quinone; FAB MS/MS, fast atom bombardment tandem mass spectrometry; 3-NBA/GLY, 3-nitrobenzyl alcohol/glycerol; OHE₁, hydroxyestron; OHE₂, hydroxyestradiol; 2-OHE₁-6-N⁶dA, N⁶-(2-hydroxyestron-6-yl)deoxyadenosine; 2-OHE₁-6-N²dG, N²-(2-hydroxyestron-6-yl)deoxyguanosine; 4-OHE₁-1(α,β)-N7Gua, 7-[4-hydroxyestron-1(α,β)-yl]guanine; 4-OHE₂-1(α,β)-N7Gua, 7-[4-hydroxyestradiol-1(α,β)-yl]guanine; LUMO, lowest unoccupied molecular orbital; Me₂SO, dimethyl sulfoxide; NOE, nuclear Overhauser effect; PDA, photodiode array; QM, quinone methide.

Scheme 1. Metabolism of Estrone and 17 β -Estradiol to *o*-Quinones

CE by horseradish peroxidase (3). In these studies, however, the structures of the adducts were not identified. Reaction of CE-Q with nucleosides would provide authentic adducts and valuable insight into the mechanism of their formation. In addition, the synthetic adducts would serve as standard compounds for elucidating adducts formed by reaction of estrogen metabolites with DNA.

In this paper the synthesis and characterization of four estrogen–nucleoside adducts formed by reaction of estrone 3,4-quinone (E_1 -3,4-Q), estradiol 3,4-quinone (E_2 -3,4-Q), or estrone 2,3-quinone (E_1 -2,3-Q) with deoxyguanosine (dG) or deoxyadenosine (dA) are reported.

Experimental Section

Caution. *Quinones of estrogen catechols are extremely toxic and were handled according to NIH guidelines (26).*

Chemicals. Synthesis of 4-OHE₁, 4-OHE₂, and 2-OHE₁ and the corresponding quinones was conducted by following the procedures of Dwivedy et al. (3). The deoxyribonucleosides dG and dA were purchased from TCI (Portland, OR) as the monohydrates and dried over P₂O₅ under vacuum at 110 °C for 48 h prior to use. All other chemicals were purchased from Aldrich Chemical Co. (Milwaukee, WI) and used without further purification.

HPLC. HPLC was conducted on a Waters 600E solvent delivery system equipped with a Waters 990 photodiode array (PDA) detector interfaced with an APC-IV Powermate computer. Analytical separations were conducted by using a YMC ODS-AQ 5- μ m, 120-Å column (6.0 \times 250 mm) at a flow rate of 1 mL/min (YMC, Morris Plains, NJ). The analytical gradient started with 30% CH₃OH in H₂O for 5 min, followed by a 60-min linear gradient (CV6) to 100% CH₃OH. Preparative HPLC was conducted by using a YMC ODS-AQ 5- μ m, 120-Å column (20 \times 250 mm) at a flow rate of 6 mL/min. The preparative gradient started with 40% CH₃OH in H₂O for 10 min, followed by a linear gradient (CV6) to 60% CH₃OH at 20 min and then held for 15 min. A linear gradient to 100% CH₃OH was then conducted for an additional 10 min, resulting in a total separation time of 45 min.

NMR. NMR spectra were recorded in dimethyl sulfoxide-*d*₆ (Me₂SO-*d*₆) at 25 °C on either a Varian XL-300 at 299.938 MHz or a Varian Unity 500 at 499.835 MHz. Chemical shifts are

reported relative to tetramethylsilane, which was employed as an internal reference. Nuclear Overhauser effect (NOE) spectra were obtained by subtracting a reference spectrum, recorded with the presaturation pulse off-resonance, from a spectrum recorded with a presaturation pulse on-resonance.

Calculations. All calculations were performed on a Silicon Graphics Iris Indigo 4000 workstation with the SYBYL 6.2 molecular modeling software (Tripos Assoc., St. Louis, MO). Structure optimization searches were performed by using the random conformation search (27) provided by SYBYL. The number of "hits" for each conformer was set to 6, ensuring a 98.4% chance of finding all possible conformations. Each conformation was then minimized by using the Tripos force field with the Powell method of convergence. Energy vs torsion angle data were obtained by the SYBYL gridsearch feature. Heats of formation were calculated with the PM3 semiempirical molecular orbital Hamiltonian (MOPAC 6.0, The Quantum Chemistry Program Exchange) (28) performed through the SYBYL interface. Optimizations used the "precise X 100" in addition to the "MMOK" keyword for molecular mechanics correction to the guanine amide bond.

Fast Atom Bombardment Tandem Mass Spectrometry (FAB MS/MS). Collisionally activated decomposition (CAD) spectra were obtained by using a VG ZAB-T, a four-sector tandem mass spectrometer of BEBE design (29). MS1 is a standard high-resolution double-focusing mass spectrometer (ZAB) of reverse geometry. MS2 has a prototype Mattauch-Herzog-type design, incorporating a standard magnet and a planar electrostatic analyzer of inhomogeneous electric field, a single-point detector, and array detector. For experiments reported here, sample quantities were sufficiently large so that the single-point detector was adequate. Samples were dissolved in 20 μ L of CH₃OH, and a 1- μ L aliquot was loaded on the probe along with 1 μ L of each matrix: a 1:1 mixture of 3-nitrobenzyl alcohol and glycerol (3-NBA/GLY), 3-NBA/GLY/LiI, or 3-NBA/GLY/NaI. A Cs⁺ ion gun operated at 30 keV was used to desorb the ions from the probe. The instrument accelerating voltage was 8 kV.

CAD spectra were obtained after precursor ion activation in the third field-free region (between MS1 and MS2). Helium was added to the collision cell (floated at 4 kV) to attenuate the ion beam by 50%. MS1 was operated at a resolving power of 1000; MS2 resolving power was set to 1000 (full width at half-height definition). Ten to fifteen 15-s scans were signal-averaged for each spectrum. Data acquisition and workup were performed

with a DEC Alpha 3000 workstation equipped with OPUS V 3.1X software and interfaced with the mass spectrometer via a VG SIOS I unit.

Exact mass measurements were conducted with a Kratos MS-50 triple analyzer tandem mass spectrometer equipped with a standard Kratos FAB source (30). The atom beam was 6–7 keV argon atoms at a total current of 1 mA at the cathode of the gun. A mixture of CsI and glycerol was used to generate reference-mass ions for the peak match mode.

Synthesis of Estrogen Nucleoside Adducts. E₁-3,4-Q or E₂-3,4-Q + dG. A suspension of 4-OHE₁ or 4-OHE₂ (0.18 mmol) in 5 mL of CH₃CN was cooled to 0 °C prior to the addition of activated MnO₂ (1.18 mmol). The suspension was stirred for 10 min and then filtered directly into a stirred solution of dG (0.94 mmol) in a solvent mixture of 10 mL of CH₃CO₂H/H₂O (1:1). Aliquots were removed for HPLC analysis at 1, 2, and 5 h to monitor the course of the reaction. After 5 h at room temperature, solvents were removed under reduced pressure and the crude product was dissolved in a 1:1 solvent mixture of CH₃OH/dimethylformamide (DMF). The product was then isolated via preparative reverse phase HPLC, as described above, to afford 7-[4-hydroxyestron-1(α,β)-yl]guanine [4-OHE₁-1(α,β)-N7Gua] or 7-[4-hydroxyestradiol-1(α,β)-yl]guanine [4-OHE₂-1(α,β)-N7Gua] (40% yield).

4-OHE₁-1(α,β)-N7Gua. ¹H and ¹³C NMR spectra showed the product to be a mixture of the designated α and β isomers; the following spectra are those of the two isomers.

UV, λ_{max} (nm): 211, 291. FTIR (KBr, cm⁻¹): 3430, 2920, 1745, 1700, 1630, 1570, 1480, 1200, 1150, 780. ¹H NMR (500 MHz): 10.72 and 10.61 (bs, 1H, 1-NH [Gua], exchanged with D₂O), 9.44 and 9.43 (bs, 1H, 3-OH, exchanged with D₂O), 8.50 and 8.49 (bs, 1H, 4-OH, exchanged with D₂O), 7.90 and 7.89 (s, 1H, 8-H [Gua]), 6.51 and 6.49 (s, 1H, 2-H), 6.14 and 6.12 (bs, 2H, 2-NH₂ [Gua], exchanged with D₂O), 2.84 (dd, *J*₁ = 17.5 Hz, *J*₂ = 4.0 Hz, 1H), 2.30–2.56 (m, 3H), 1.96–2.02 (m, 1H), 1.83–1.90 (m, 2H), 1.23–1.61 (m, 4H), 1.10–1.21 (m, 1H), 0.74–0.98 (m, 2H), 0.74 (s, 3H, 13-CH₃), 0.45–0.68 (m, 1H). ¹³C NMR (75 MHz): 162.2, 160.2, 159.9, 153.9, 153.8, 152.9, 152.8, 143.5, 143.2, 143.0, 142.8, 142.1, 142.0, 127.4, 126.3, 126.1, 125.8, 125.7, 113.6, 112.8, 109.3, 108.0, 49.7, 49.4, 47.3, 47.2, 44.2, 43.7, 35.7, 35.1, 32.3, 31.8, 30.7, 25.2, 25.1, 24.4, 24.3, 24.2, 21.1, 13.7, 13.6. MS, (M + H)⁺ C₂₃H₂₆N₅O₄ calcd 436.19850, found 436.19863.

4-OHE₂-1(α,β)-N7Gua. ¹H NMR spectrum showed the product to be a mixture of the α and β isomers; the following spectra are those of the two isomers.

UV, λ_{max} (nm): 211, 292. ¹H NMR (500 MHz): 10.72 and 10.64 (bs, 1H, 1-NH [Gua], exchanged with D₂O), 9.38 and 9.36 (bs, 1H, 3-OH, exchanged with D₂O), 8.44 and 8.43 (bs, 1H, 4-OH, exchanged with D₂O), 7.89 and 7.88 (s, 1H, 8-H [Gua]), 6.48 and 6.46 (s, 1H, 2-H), 6.13 and 6.11 (bs, 2H, 2-NH₂ [Gua], exchanged with D₂O), 4.39 and 4.35 (d, *J* = 3.7 Hz, 1H, 17β-OH), 4.08 (m, 1H, 17α-H), 2.79 (dd, *J*₁ = 17.0 Hz, *J*₂ = 4.0 Hz, 1H), 2.30–2.56 (m, 3H), 1.75–1.87 (m, 1H), 1.66–1.75 (m, 1H), 1.46–1.57 (m, 1H), 1.16–1.42 (m, 4H), 0.74 (s, 3H, 13-CH₃), 0.48–0.58 (m, 1H). MS, (M + H)⁺ C₂₃H₂₈N₅O₄ calcd 438.21410, found 438.21410.

E₁-2,3-Q + dA. A suspension of 2-OHE₁ (0.18 mmol) in 5 mL CH₃CN was cooled to –40 °C prior to the addition of activated MnO₂ (1.18 mmol). The suspension was stirred for 10 min and then filtered directly into a stirred solution of dA (0.94 mmol) in a solvent mixture of 10 mL of CH₃CO₂H/H₂O (1:1). Aliquots were removed for HPLC analysis at 1, 2, and 5 h to monitor the course of the reaction. After 5 h at room temperature, solvents were removed under reduced pressure, and the crude product was dissolved in a 1:1 solvent mixture of CH₃OH/DMF. The product was then isolated via preparative reverse phase HPLC, as described above, to afford N⁶-(2-hydroxyestron-6-yl)deoxyadenosine (2-OHE₁-6-N⁶dA) (80% yield).

2-OHE₁-6-N⁶dA. UV, λ_{max} (nm): 207, 276. ¹H NMR (300 MHz): 8.61 (s, 1H, OH, exchanged with D₂O), 8.57 (s, 1H, OH, exchanged with D₂O), 8.31 and 8.27 (s and bs, 2H, 2-H and 8-H [dA]), 7.94 (d, 2H, *J* = 9.0 Hz, 6-NH [dA], exchanged with D₂O),

6.68 (s, 1H, 1-H), 6.56 (s, 1H, 4-H), 6.36 (t, 1H, *J* = 6.7 Hz, 1'-H [dA]), 5.58 (m, 1H, 6-H), 5.27 (d, 1H, *J* = 4.1 Hz, 3'-OH [dA], exchanged with D₂O), 5.17 (t, 1H, *J* = 6.0 Hz, 5'-OH [dA], exchanged with D₂O), 4.41 (m, 1H, 3'-H [dA]), 3.88 (m, 1H, 4'-H [dA]), 3.45–3.59 (m, 2H, 5'-H₂ [dA]), 2.73 (q, *J* = 6.5 Hz, 1H), 2.38 (dd, *J*₁ = 18.5 Hz, *J*₂ = 7.5 Hz, 1H), 2.19–2.27 (m, 2H), 1.90–2.16 (m, 4H), 1.84 (t, *J* = 9.0 Hz, 1H), 1.73–1.78 (m, 1H), 1.56–1.67 (m, 1H), 1.34–1.49 (m, 3H), 0.81 (s, 3H, 13-CH₃). MS, (M + H)⁺ C₂₈H₃₄N₅O₆ calcd 536.25090, found 536.25117.

E₁-2,3-Q + dG. A suspension of 2-OHE₁ (0.25 mmol) in 5 mL of CH₃CN was cooled to –40 °C prior to the addition of activated MnO₂ (2.25 mmol). The suspension was stirred for 10 min and then filtered directly into a stirred solution of dG (1.30 mmol) in a solvent mixture of 10 mL of CH₃CO₂H/H₂O (1:1). Aliquots were removed for HPLC analysis at 1, 2, and 5 h to monitor the course of the reaction. After 5 h at room temperature, solvents were removed under reduced pressure, and the crude product was dissolved in a 1:1 solvent mixture of CH₃OH/DMF. The product was then isolated via preparative reverse phase HPLC, as described above, to afford N²-(2-hydroxyestron-6-yl)deoxyguanosine (2-OHE₁-6-N²dG) (10% yield).

2-OHE₁-6-N²dG. UV, λ_{max} (nm): 254, 287. ¹H NMR (500 MHz): 9.92 (bs, 1H, 1-NH [dG], exchanged with D₂O), 8.83 (bs, 2H, 2-OH and 3-OH, exchanged with D₂O), 7.91 (s, 1H, 8-H [dG]), 6.84 (d, 1H, 2-NH [dG], exchanged with D₂O), 6.69 (s, 1H, 1-H), 6.64 (s, 1H, 4-H), 6.18 (t, 1H, *J* = 6.7 Hz, 1'-H [dG]), 5.29 (d, 1H, *J* = 4.0 Hz, 3'-OH [dG], exchanged with D₂O), 4.99 (m, 1H, 6-H), 4.87 (t, 1H, *J* = 6.0 Hz, 5'-OH [dG], exchanged with D₂O), 4.38 (m, 1H, 3'-H [dG]), 3.81 (m, 1H, 4'-H [dG]), 3.49–3.58 (m, 2H, 5'-H₂ [dG]), 2.71 (q, *J* = 6.5 Hz, 1H), 2.41 (dd, *J*₁ = 18.0 Hz, *J*₂ = 7.0 Hz, 1H), 2.16–2.28 (m, 2H), 1.98–2.22 (m, 3H), 1.85–1.96 (m, 1H), 1.32–1.18 (m, 6H), 0.85 (s, 3H, 13-CH₃). MS, (M + H)⁺ C₂₈H₃₄N₅O₇ calcd 552.24580, found 552.24607.

Results

Synthesis and Structure Determination of Estrogen Quinone Adducts Formed with Deoxyribonucleosides. Initial attempts to synthesize nucleoside adducts of estrogen quinones in aprotic solvents yielded no adducts. Neither dG nor dA reacted with E₁-3,4-Q or E₁-2,3-Q in DMF or Me₂SO. In acidic conditions, however, reaction of estrogen quinones with sulfur nucleophiles was previously reported (31). The solvent system to CH₃CO₂H/H₂O (1:1) facilitated Michael addition of nucleophilic groups in dG and dA to both E₁-3,4-Q and E₁-2,3-Q, to give the products shown in Scheme 2. No adducts were obtained with deoxycytidine or thymidine. The quinones were formed in CH₃CN at 0 °C for 4-OHE₁ and 4-OHE₂ and at –40 °C for 2-OHE₁ (3) and then filtered directly into a solution of the nucleoside previously dissolved in the 1:1 mixture of CH₃CO₂H/H₂O (ca. pH 2).

Reaction of E₁-3,4-Q with dG yielded a product that eluted as a single peak under several different HPLC conditions. Reaction yields were typically 40%. The reaction proceeded to completion after 5 h at room temperature, and no other adducts were detected. NMR analysis (detailed discussion below) showed the product to be a mixture of two conformational isomers attached to the C1 position of the estrogen A ring and the N7 position of guanine, 4-OHE₁-1(α,β)-N7Gua. The generation of two conformational isomers is the result of a rotational barrier about the C1–N7Gua bond. Thus, in one isomer, the guanine moiety is located primarily on the “α” side of the estrogen ring system, 4-OHE₁-1α-N7Gua, while the other isomer has the guanine moiety located on the “β” side of the estrogen ring system, 4-OHE₁-1β-N7Gua (Figure 1). Rotation from the α isomer to the β isomer would involve the C8-Gua proton

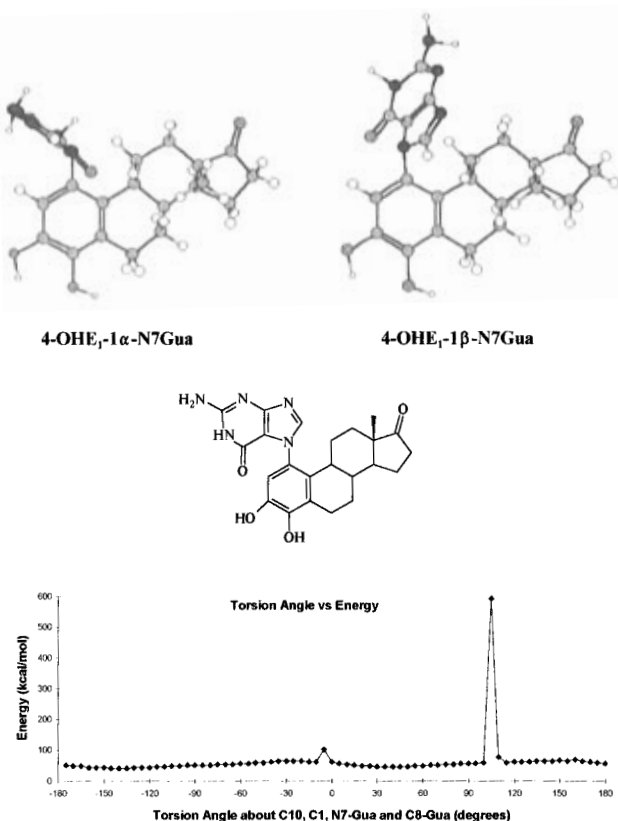
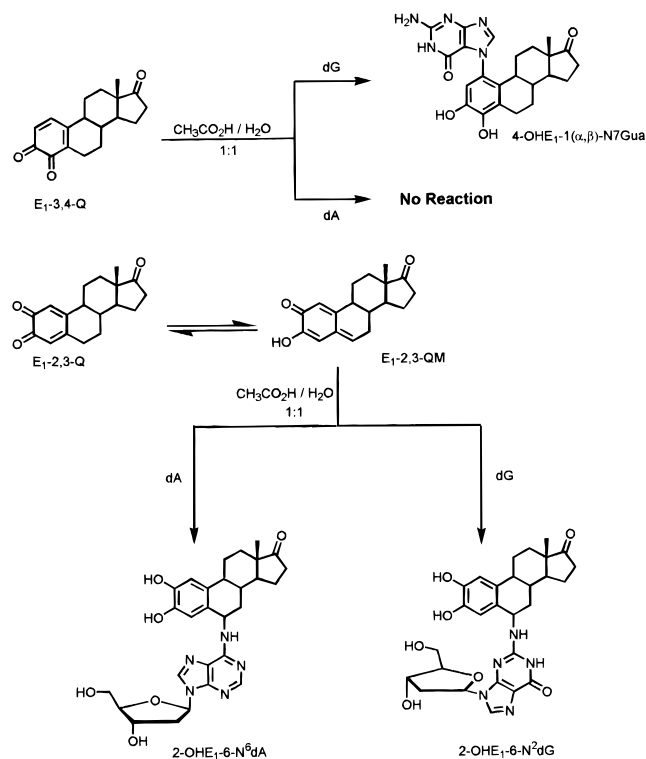


Figure 1. Structure of 4-OHE₁-1 α -N7Gua and 4-OHE₁-1 β -N7Gua along with a graph of energy vs torsion angle (C10, C1, N7Gua, and C8Gua).

Scheme 2. Reaction of Estrogen Quinones with dG and dA



occupying the same van der Waals radius as the C11 protons of the estrogen B ring. A graph of energy as a function of the torsion angle about C10, C1, N7-Gua, and C8-Gua (Figure 1) shows a rotation barrier of 551 kcal/mol. The two isomers were formed in a ratio (via ¹H

NMR) of 60% β and 40% α (assignment of the α and β isomers is discussed below). The predominance of the β isomers indicates formation of this adduct is under kinetic control, since calculations show the α isomer is thermodynamically more stable than the β isomer. Molecular mechanical calculations, $\Delta E_{\alpha,\beta} = -5.9$ kcal/mol, and semiempirical quantum mechanical calculations, $\Delta H_{\alpha,\beta} = -2.9$ kcal/mol, show the α isomer to be the more stable form. Attack of the nitrogen nucleophile at C1 is the result of a 1,4-addition with respect to the C3 carbonyl. This is in contrast to sulfur nucleophiles, which attack at the C2 position, a 1,6-addition with respect to the C4 carbonyl (31). Molecular orbital calculations (semiempirical, PM3 Hamiltonian) (28) have shown that, in the neutral species, C1 bears more positive charge than C2 and that the lowest unoccupied molecular orbital (LUMO) has a higher coefficient at C2 than C1.² Thus, soft electrophiles, such as thiols, will attack at C2 (32), while harder electrophiles, such as nitrogen and oxygen, will attack C1.² When molecular orbital calculations are done on protonated E₁-3,4-Q (i.e., acidic conditions), the regioselective attack on C1 by hard electrophiles is enhanced.²

E₁-3,4-Q did not react with dA. With this nucleoside, only gradual decomposition of the quinone was observed. Reaction of E₂-3,4-Q with dG and dA produced the same results as E₁-3,4-Q.

Reaction of E₁-2,3-Q with dG yielded the product 2-OHE₁-6-N⁶dG. The product is a result of 1,6-addition to the quinone after initial tautomerization of E₁-2,3-Q to the quinone methide (QM; Scheme 2). The reaction yield was low, ca. 10%. Reaction of E₁-2,3-Q with dA produced a similar product, 2-OHE₁-6-N⁶dA, but in much higher yields of 80%. Recently, investigation into the isomerization of *o*-quinones to quinone methides has been published (33, 34). The *o*-quinone of 2,3-dihydroxy-5,6,7,8-tetrahydronaphthalene, in which the A, B rings are equivalent to 2-OHE₁, was shown to be more stable by 3.8 kcal/mol when tautomerized to the QM (34). Although the *o*-quinone is formed initially, it isomerizes to the more electrophilic QM upon standing in CH₃CN for extended periods of time (34). Calculations on thermodynamic energies of E₁-2,3-Q and E₁-2,3-QM6 show they are very close in energy. Molecular mechanical calculations show the QM more stable by 0.3 kcal/mol, while quantum mechanical calculations (semiempirical, PM3 Hamiltonian) reveal the *o*-quinone to be more stable by 1.3 kcal/mol. To study the possibility of E₁-2,3-Q to E₁-2,3-QM tautomerization, E₁-2,3-Q was generated in CH₃CN-*d*₃ and its ¹H NMR spectrum was monitored over time. The initial spectrum showed the presence of only the *o*-quinone, and the spectrum remained unchanged for 2 days. Even with the addition of CF₃CO₂H-*d* to help catalyze the tautomerization, no change in the *o*-quinone spectrum was observed after standing for 2 weeks. This experiment indicates that in CH₃CN the *o*-quinone form of E₁-2,3-Q is more stable. However, reaction of E₁-2,3-Q with dG and dA resulted in 6-substituted products, indicating that only the E₁-2,3-QM isomer, present in small quantities, reacts with these nucleosides.

Because acidic conditions were used to generate these estrogen-nucleoside adducts, an investigation was conducted of the effects of pH on the stability of both the

² Unpublished results (D. Stack and E. Cavalieri).

Table 1. Stability of E₁-3,4-Q and E₁-2,3-Q at Various pH

pH ^a	<i>t</i> _{1/2} (min) ^b	
	E ₁ -3,4-Q ^{c,d}	E ₁ -2,3-Q ^e
9	<5	<5
7	110	110
5	190	110
3	390	70

^a pH was adjusted with the following 0.1 M buffers: pH 9, Tris-HCl; pH 7, distilled H₂O; pH 5, Trizma; pH 3, citric acid. ^b *t*_{1/2} is defined as the time when 1/2 of the original quinone concentration was observed by HPLC. The original concentration was established by injection of an aliquot of the original quinone solution (0.02 mmol in CH₃CN). ^c Quinones (0.02 mmol) were synthesized in 2 mL of CH₃CN and placed in 10 mL of aqueous buffer. ^d Sampling times (min) are as follows: pH 3: 56, 156, 206, 306, 356, 406; pH 5: 65, 125, 185, 245, 305; pH 7: 5, 40, 80, 130, 190; pH 9: 5. ^e Sampling times (min) are as follows: pH 3: 35, 85, 135, 185; pH 5: 3, 53, 158, 208; pH 7: 15, 30, 50, 95, 195; pH 9: 5.

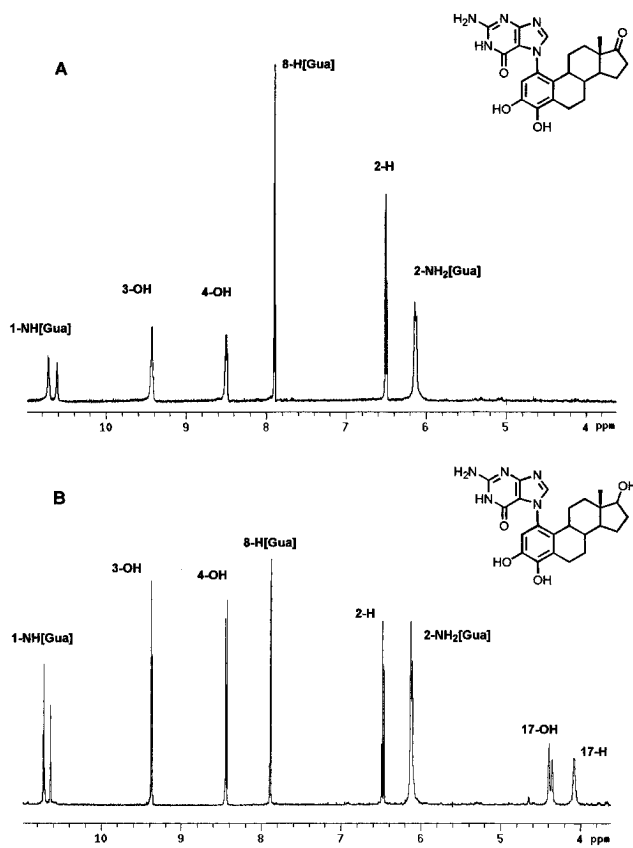


Figure 2. NMR spectra of the (A) 4-OHE₁-1(α,β)-N7Gua and (B) 4-OHE₂-1(α,β)-N7Gua adducts.

3,4- and 2,3-quinones. E₁-3,4-Q showed a marked increase in stability as the pH was lowered from 7 to 3 (Table 1), whereas E₁-2,3-Q did not. The 3,4- and 2,3-quinones decomposed rapidly under mildly basic conditions. Both quinones were relatively stable, with a *t*_{1/2} of 110 min at pH 7, indicating a prolonged presence, if formed *in vivo*.

(A) 4-OHE₁-1(α,β)-N7Gua. In the NMR spectrum of 4-OHE₁-1-N7Gua (Figure 2A), the presence of two sets of peaks indicates a mixture of two distinct chemical species. One isomer is formed in greater amount, approximately 60:40. Initially, a mixture of regioisomers at the C1 and C2 positions formed by attack of the N7 of dG was thought to account for the two chemical species. However, careful analysis by NOE showed that the N7 of guanine is bonded at the C1 position in both isomers, 4-OHE₁-1(α,β)-N7Gua (Figure 1). NOE effects between

the C1 proton and the C11 protons have been demonstrated for the parent compound, 4-OHE₁, and other estrogen adducts substituted at C2 (35). No NOE effect was seen between the resonance signals at 6.51/6.49 ppm (2-H) and other protons in the aliphatic region. Moreover, a strong NOE effect was seen between the 3-OH proton (9.44 and 9.43 ppm) and both resonance signals at 6.51 and 6.49 ppm. A significant upfield shift of several aliphatic protons, 1.10–1.21 (m, 1H), 0.74–0.98 (m, 2H), 0.45–0.68 (m, 1H), was also observed (not shown), whereas the parent compound, 4-OHE₁, has no protons in this region (with the exclusion of the 13-CH₃ singlet). These protons are likely to be the ones at C11 or C12 since perpendicular attachment at C1 of the guanine ring (Figure 1) would produce shielding to these protons. A similar upfield shift has been seen for adenine and guanine adducts at C-12 in the benz[*a*]anthracene compounds (36). Loss of the deoxyribose moiety is evidence for nucleophilic attack at N7 of dG. In fact, substitution at N7 destabilizes the glycosidic bond (36–38), resulting in the loss of deoxyribose and its signals in the aliphatic region of the NMR spectrum. The presence of the 2-NH₂ proton resonance at 6.12 ppm, as well as the C-8 proton resonance at 7.90 ppm (Figure 2A), indicates that these two nucleophilic sites in the guanine moiety are not substituted, thereby corroborating substitution at N7. ¹³C NMR also confirmed the presence of two isomers. One isomer would generate 11 carbon signals in the aromatic region, but 22 were observed. In the aliphatic region, 12 signals would be seen if one isomer were present, but 19 were observed, with 5 carbon atoms of the two isomers having the same chemical shift.

Additional NOE experiments allowed not only the validation of two conformational isomers, but also assignment of the α and β forms. Molecular modeling (Figure 1) showed that the distance between the proton on C2 and C8-Gua differs between the α and β isomers, 3.03 and 4.23 Å, respectively. However, the distance between the protons on 3-OH and C2 are very similar, 3.60 and 3.62 Å, respectively. Therefore, the NOE between the protons on C2 and C8-Gua, via irradiation of the C8-Gua protons, should change the ratio of the C2 protons in the NOE difference spectrum. In contrast, the NOE effect between the protons on 3-OH and C2, via irradiation of the 3-OH protons, should be equal between the α and β isomers, and consequentially, the ratio of the C2 protons should remain unchanged. Three sets of NOE spectra are shown in Figure 3, with the “normal” 1D spectrum (presaturation off-resonance) placed above the difference spectrum displaying the NOE effect. When the 3-OH proton (9.44 and 9.43 ppm) is irradiated, the NOE effect seen on the C2 protons gives the same ratio between the resonance signals at 6.51 and 6.49 ppm (Figure 3A). When the C8-Gua proton (7.91 and 7.90 ppm) is irradiated, the ratio of the two peaks changes such that the peak at 6.49 is now the major peak (Figure 3B) and hence belongs to the α isomer since the distance between these protons is smaller than that of the β isomer. When the C2 proton (6.51 and 6.49 ppm) is irradiated, the ratio of the 3-OH protons (9.44 and 9.43 ppm) remains unchanged, while the ratio of the C8-Gua protons (7.91 and 7.90 ppm) is reversed such that the peak at 7.91 ppm (α isomer) is predominant (Figure 3C). Thus, the major isomer is the β form.

FAB of 4-OHE₁-1(α,β)-N7Gua produces an [M + H]⁺ ion of *m/z* 436 and an [M + Li]⁺ ion of *m/z* 442. The exact mass is consistent with the proposed elemental

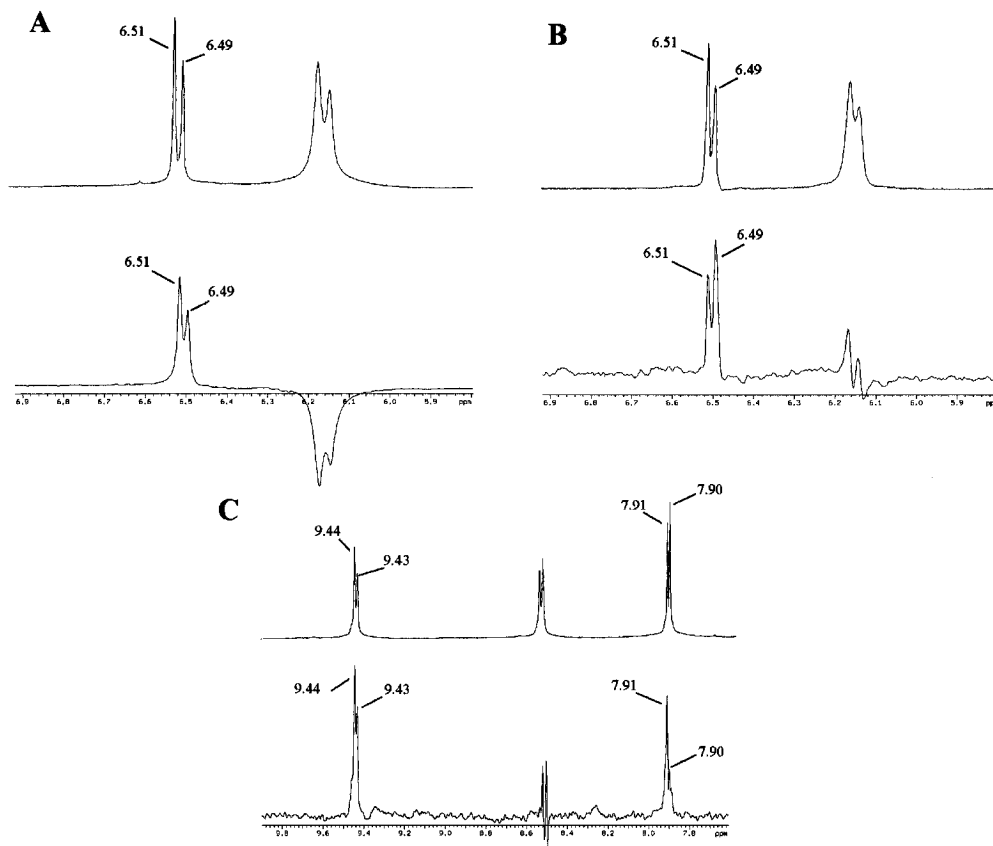


Figure 3. Determination of α and β isomers of 4-OHE₁-1-N7Gua by NOE irradiation. (A) Top spectrum: 1D with presaturation off-resonance. Bottom spectrum: NOE difference spectrum, irradiation of the 3-OH proton (9.44 and 9.43 ppm). (B) Top spectrum: 1D with presaturation off-resonance. Bottom spectrum: NOE difference spectrum, irradiation of the C8-Gua proton (7.91 and 7.90 ppm). (C) Top spectrum: 1D with presaturation off-resonance. Bottom spectrum: NOE difference spectrum, irradiation of the C2 proton (6.51 and 6.49 ppm).

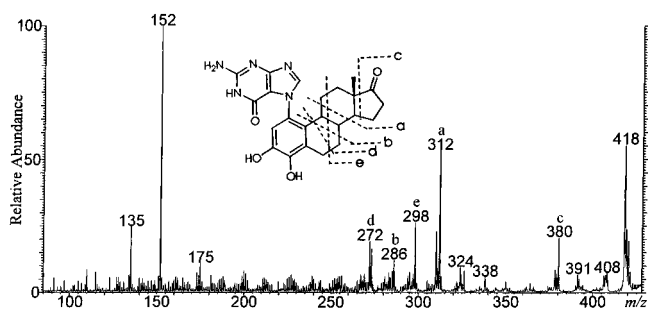


Figure 4. Portion of the CAD mass spectrum of $[M + H]^+$ ion of m/z 436 from 4-OHE₁-1(α,β)-N7Gua.

composition. CAD spectra of the $[M + H]^+$ and $[M + Li]^+$ ions were investigated to obtain molecular structure information. Upon collisional activation, the $[M + H]^+$ ions decompose to form major fragment ions of m/z 418 ($M + H - H_2O$)⁺, m/z 380 ($C_{20}H_{22}O_3N_5$)⁺, m/z 312 ($C_{15}H_{14}O_3N_5$)⁺, m/z 298 ($C_{14}H_{12}O_3N_5$)⁺, m/z 286 ($C_{13}H_{12}O_3N_5$)⁺, m/z 272 ($C_{12}H_{10}O_3N_5$)⁺, m/z 152 (Gua + H)⁺, and m/z 135 (Gua + H - NH₃)⁺ (Figure 4). The $[M + Li]^+$ ions dissociate to produce similar fragment ions as for the $[M + H]^+$ ions, except those ions containing the guanine moiety shift by six mass units to higher mass.

A few fragment ions are formed by simple cleavage at a protonated site. The ion of m/z 418 is formed by the loss of a water molecule presumably upon protonation of an OH group. The ion of m/z 152, which is strong evidence for the presence of guanine, is produced by protonation at N7 of the guanine, followed by hydride rearrangement and cleavage of the C-N bond. An

analogous ion is observed at m/z 158 in the CAD spectrum of the $[M + Li]^+$ ion, suggesting that the lithium is bound to the nucleobase in the precursor ion.

Because the bonding of the nucleobase and steroid is strong, most fragment ions are generated by charge-remote cross-ring cleavages (Figure 4), as was previously established for simpler steroids (39). The m/z 312 ion is formed by the loss of $C_8H_{12}O$ from charge-remote cleavages of the C9-C11 and C8-C14 bonds. The other fragment ions at m/z 380, 312, and 272 are also produced by two ring C-C bond cleavages. The ion of m/z 286 is formed by two-bond cleavages; it is not, however, the radical cation of the steroid, as was expected on the basis of the CAD spectra of polycyclic aromatic hydrocarbon adducts (36-38). The formation of the ion of m/z 298 is more complex and is initiated by ring opening of the C ring, followed by hydrogen rearrangement from the hydroxy group at C-4 of the A ring and loss of $C_9H_{14}O$.

(B) 4-OHE₂-1(α,β)-N7Gua. The NMR spectrum of 4-OHE₂-1(α,β)-N7Gua (Figure 2B) is similar to that of 4-OHE₁-1(α,β)-N7Gua, with the addition of signals for the 17 α -proton at 4.08 ppm and the 17 β -OH proton at 4.38 ppm.

FAB of 4-OHE₂-1(α,β)-N7Gua produces an $[M + H]^+$ species of m/z 438 and an $[M + Li]^+$ ion of m/z 444. The exact mass is consistent with the proposed elemental composition. CAD spectra of the $[M + H]^+$ and $[M + Li]^+$ ions contain a series of ions of the same mass as observed in the CAD spectra of the $[M + H]^+$ and $[M + Li]^+$ ions, respectively, of 4-OHE₁-1(α,β)-N7Gua, supporting the hypothesis that the charge is localized on the DNA base and the fragmentations occur at the B, C, and D rings

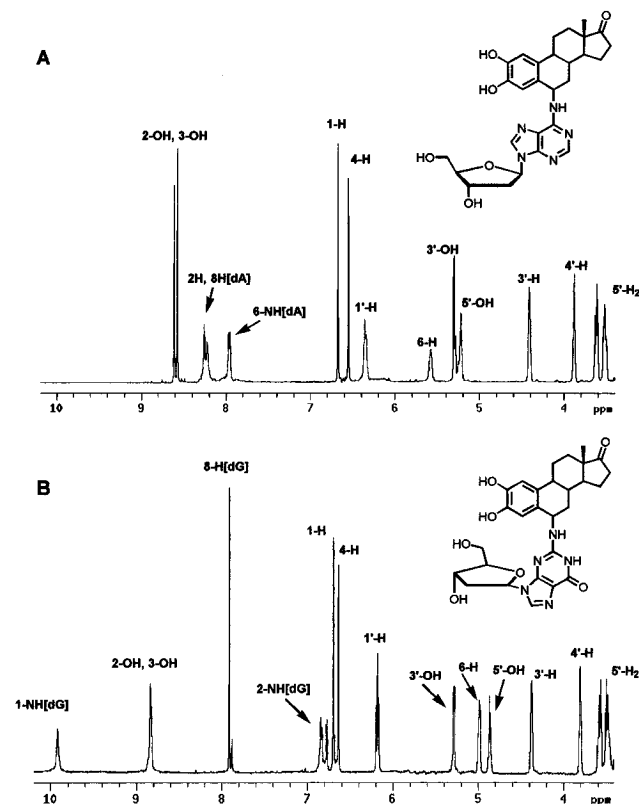


Figure 5. NMR spectra of the (A) 2-OHE₁-6-N²dG and (B) 2-OHE₁-6-N⁶dA adducts.

remote from the charge site. Exceptions may be ions formed by losses of water.

(C) 2-OHE₁-6-N⁶dA. Two key structural features are reflected in the NMR spectrum of 2-OHE₁-6-N⁶dA (Figure 5A). First, the presence of the aliphatic signals corresponding to the deoxyribose moiety suggests substitution at the 6-NH₂ position of dA, because substitution at the other two nucleophilic groups of dA, N-3 and N-7, leads to loss of the deoxyribose moiety by depurination (36–38). This is confirmed by the lack of the signals at 7.33 corresponding to the 6-NH₂ in dA (not shown). Instead, a doublet is found at 7.94 ppm (exchangeable with D₂O) that corresponds to the 6-NH group attached to the C-6 position of the 2-OHE₁ moiety. Evidence for substitution at C-6 is derived from the two-dimensional chemical shift correlation spectroscopy technique, which shows the C-6 proton resonance at 5.58 ppm coupled with the 6-NH (dA) proton at 7.94 ppm. Signals for both the 1- and 4-protons on the A ring are still present, further supporting the proposed structure. The protons at C-6 are prochiral, and attack of the dA nucleophile leads to a mixture of diastereoisomers in a ratio of 4:1. However, assignment of the two diastereoisomers has yet to be established.

FAB of 2-OHE₁-6-N⁶dA generates an [M + H]⁺ species of *m/z* 536 and an [M + Na]⁺ ion of *m/z* 558. Upon collisional activation, the [M + H]⁺ ion yields diagnostic fragment ions of *m/z* 420, 285, 252, 136, and 117 (Figure 6). The fragment ion of *m/z* 420 is produced by hydrogen transfer from the deoxyribose to the adenine moiety, followed by elimination of C₅H₈O₃. This ion is formally the [M + H]⁺ species of the modified base. The formation of the ion of *m/z* 285, which is the 2-OHE₁ cation, results from the cleavage between the benzylic C-6 of the 2-OHE₁ moiety and the N⁶ of the exocyclic amino group of dA, whereas the ion of *m/z* 252, protonated dA, is produced by the same bond cleavage with hydrogen rearrangement

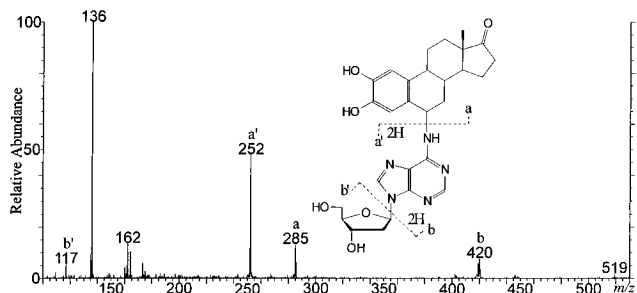


Figure 6. The CAD mass spectrum of [M + H]⁺ ion of *m/z* 536 from 2-OHE₁-6-N⁶dA.

to the nucleobase. The product ions of *m/z* 136 and 117 are protonated adenine and deoxyribose, respectively. Collisional activation of the ion of *m/z* 420, which is the protonated 2-OHE₁-Ade adduct without the ribose, generates three major fragment ions at *m/z* 403 (by loss of NH₃), 285 (2-OHE₁ carbocation), and 136 (protonated adenine). No ion for the deoxyribose (*m/z* 117) moiety was observed.

The CAD spectrum of the [M + Na]⁺ ion was examined to determine the location of the charge site of this adduct when the sample desorbs upon FAB. The major CAD is the formation of [Ade + Na]⁺ at *m/z* 157. As observed for OHE₁ and OHE₂ adducts, other fragment ions that contain the nucleobase shift by 22 mass units, suggesting that the sodium ion (like the lithium ion in the previous examples) is bound to the adenine.

(D) 2-OHE₁-6-N²dG. The NMR spectrum of 2-OHE₁-6-N²dG (Figure 5B) is similar to that of the 2-OHE₁-6-N⁶dA with signals corresponding to the deoxyribose moiety, the C-1 and C-4 protons of the A ring, and the 2-NH of dG coupled to the C-6 position of the B ring. Again, attack at the prochiral C-6 results in formation of two diastereoisomers.

FAB of 2-OHE₁-6-N²dG produces two major ions of *m/z* 552 [M + H]⁺ and of *m/z* 436 (protonated 2-OHE₁-6-N²-Gua). The latter ion arises by hydrogen transfer from the sugar moiety to the base, followed by elimination of C₅H₈O₃. The ion of *m/z* 574 [M + Na]⁺ is also present in the spectrum. Collisional activation of the ion of *m/z* 574 produces three major fragment ions at *m/z* 458 [modified Gua + Na]⁺, 290 [Gua + deoxyribose + Na]⁺, and 174 [Gua + Na]⁺. The metal ion binds to the nucleobase as in the dA adduct. The CAD spectrum of the [M + H]⁺ ion contains diagnostic fragment ions of *m/z* 436 (modified Gua), 285 (2-OHE₁ cation), 268 (protonated dG), 152 [Gua + H]⁺, and 117 (deoxyribose moiety). Most fragment ions are produced by simple cleavage, often accompanied by hydrogen rearrangement. The ion of *m/z* 436 is collisionally dissociated to give two distinctive fragments: protonated Gua and the 2-OHE₁ carbocation.

Discussion

The catechol pathway in the metabolism of estrogens can lead to ultimate carcinogenic species, namely, the catechol estrogen quinones. The reaction of E₁-2,3-Q, E₁-3,4-Q, and E₂-3,4-Q with deoxyribonucleosides has been investigated with the purpose of providing insight into the possible modes of binding of these intermediates to DNA. At the same time, authentic adducts have been prepared for use as standards in the elucidation of the

structure of biologically-formed DNA adducts.

The 2,3- and 3,4-quinones display different chemistry toward the nucleophiles dG and dA. The most striking feature, with implication for DNA damage, is that the 3,4-quinones form N7Gua adducts in which the glycosidic bond of dG is destabilized, leading to formation of the E₁- or E₂-1(α,β)-N7Gua adducts. In contrast, the 2,3-quinones bind at the exocyclic amino group of dG or dA, allowing the deoxyribose moiety to remain attached to the adduct.

These results have several implications for DNA damage. First, the *o*-quinones of estrogens are capable of binding directly to the nucleophilic groups of DNA bases; second, the 3,4-quinones of estrogens produce depurinating adducts that are lost from DNA, generating apurinic sites in the DNA; and third, the 2,3-quinones form stable adducts that remain bound to DNA if not repaired. In fact, reaction of 2,3- and 3,4-quinones with DNA or CE activated by horseradish peroxidase in the presence of DNA affords differential formation of stable adducts, as evidenced by ³²P-postlabeling analysis (3). The 2,3-quinones form 10–50 times higher levels of stable adducts than the 3,4-quinones. The 3,4-quinones and the enzymically-activated 4-OHE₁ and 4-OHE₂ form almost exclusively the depurinating E₁(E₂)-1(α,β)-N7Gua adducts both *in vitro* and in the rat mammary gland.³

In the hamster kidney tumor model, 4-OHE₁ and 4-OHE₂ are carcinogenic, whereas the corresponding 2-OH isomers are not (17, 18). The elevated expression of estrogen 4-hydroxylase activity in human and animal tissues susceptible to estrogen-induced tumors (5, 19–25) is a further indication that the 4-catechol pathway may be involved in tumor initiation by estrogens. The carcinogenicity of the 4-OH estrogens may be explained by the formation of depurinating adducts with the 3,4-quinones. This activity contrasts with the noncarcinogenicity of the 2-OH estrogens, which form only stable adducts. A similar relationship has been established between formation of depurinating DNA adducts by polycyclic aromatic hydrocarbons and induction of oncogenic mutations in mouse skin papillomas induced by these compounds (40).

In conclusion, the adducts described here provide insight into the type of DNA damage possible when CE-Q are generated *in vitro* and *in vivo* and will be used in studies designed to elucidate the structure of estrogen adducts in biological systems.

Acknowledgment. We thank Drs. S.-T. Jan and P. Mulder for synthesis of catechol estrogens. Molecular modeling studies were conducted in the Molecular Modeling Core Facility, UNMC/Eppley Cancer Center. We gratefully acknowledge support from USPHS Grant P01 CA49210 and NRSA 1F32 CA65084. Core support for the Eppley Institute was provided by Grant CA36727 from the National Cancer Institute. The Washington University Mass Spectrometry Resource is supported by the NIH National Center for Research Resources (Grant 2P41RR00954).

References

- (1) Nandi, S., Guzman, R. C., and Yang, J. (1995) Hormones and mammary carcinogenesis in mice, rats, and humans: A unifying hypothesis. *Proc. Natl. Acad. Sci. U.S.A.* **92**, 3650–3657.
- (2) Liehr, J. G. (1990) Genotoxic effects of estrogens. *Mutat. Res.* **238**, 269–276.
- (3) Dwivedy, I., Devanesan, P., Cremonesi, P., Rogan, E., and Cavalieri, E. (1992) Synthesis and characterization of estrogen 2,3- and 3,4-quinones. Comparison of DNA adducts formed by the quinones versus horseradish peroxidase-activated catechol estrogens. *Chem. Res. Toxicol.* **5**, 828–833.
- (4) Ball, P., and Knuppen, R. (1980) Catechol oestrogens (2- and 4-hydroxyestrogens): Chemistry, biogenesis, metabolism, occurrence and physiological significance. *Acta Endocrinol. (Copenhagen)* **93** (Suppl. 232), 1–127.
- (5) Zhu, B. T., Bui, Q. D., Weisz, J., and Liehr, J. G. (1994) Conversion of estrone to 2- and 4-hydroxyestrone by hamster kidney and liver microsomes: Implications for the mechanism of estrogen-induced carcinogenesis. *Endocrinology* **135**, 1772–1779.
- (6) Kalyanaraman, B., Sealy, R. C., and Sivarajah, K. (1984) An electron spin resonance study of *o*-semiquinones formed during the enzymatic and autoxidation of catechol estrogens. *J. Biol. Chem.* **259**, 14018–14022.
- (7) Kalyanaraman, B., Felix, C. C., and Sealy, R. C. (1985) Semiquinone anion radicals of catechol (amine)s, catechol estrogens, and their metal ion complexes. *Environ. Health Perspect.* **64**, 185–198.
- (8) Liehr, J. G., Ulubelen, A. A., and Strobel, H. W. (1986) Cytochrome P-450-mediated redox cycling of estrogens. *J. Biol. Chem.* **261**, 16865–16870.
- (9) Roy, D., Bernhardt, A., Strobel, H. W., and Liehr, J. G. (1992) Catalysis of the oxidation of steroid and stilbene estrogens to estrogen quinone metabolites by the beta-naphthoflavone-inducible cytochrome P450 IA family. *Arch. Biochem. Biophys.* **296**, 450–456.
- (10) Liehr, J. G., and Roy, D. (1990) Free radical generation by redox cycling of estrogens. *Free Radical Biol. Med.* **8**, 415–423.
- (11) Liehr, J. G. (1994) Mechanisms of metabolic activation and inactivation of catecholestrogens: A basis of genotoxicity. *Polycyclic Aromat. Compd.* **6**, 229–239.
- (12) Nutter, L. M., Ngo, E. O., and Abul-Hajj, Y. J. (1991) Characterization of DNA damage induced by 3,4-estrone-*o*-quinone in human cells. *J. Biol. Chem.* **266**, 16380–16386.
- (13) Nutter, L. M., Wu, Y.-Y., Ngo, E. O., Sierra, E. E., Gutierrez, P. L., and Abul-Hajj, Y. J. (1994) An *o*-quinone form of estrogen produces free radicals in human breast cancer cells: Correlation with DNA damage. *Chem. Res. Toxicol.* **7**, 23–28.
- (14) Li, J. J., Li, S. A., Klicka, J. K., Parsons, J. A., and Lam, L. K. T. (1983) Relative carcinogenic activity of various synthetic and natural estrogens in the Syrian hamster kidney. *Cancer Res.* **43**, 5200–5204.
- (15) Kirkman, H. (1959) Estrogen-induced tumors of the kidney in the Syrian hamster. *Natl. Cancer Inst. Monogr.* **No. 1**, 1–59.
- (16) Liehr, J. G. (1983) 2-Fluoroestradiol: Separation of estrogenicity from carcinogenicity. *Mol. Pharmacol.* **23**, 278–281.
- (17) Liehr, J. G., Fang, W. F., Sirbasku, D. A., and Ari-Ulubelen, A. (1986) Carcinogenicity of catechol estrogens in Syrian hamsters. *J. Steroid. Biochem.* **24**, 353–356.
- (18) Li, J. J., and Li, S. A. (1987) Estrogen carcinogenesis in Syrian hamster tissues: Role of metabolism. *Fed. Proc.* **46**, 1858–1863.
- (19) Weisz, J., Bui, Q. D., Roy, D., and Liehr, J. G. (1992) Elevated 4-hydroxylation of estradiol by hamster kidney microsomes: A potential pathway of metabolic activation of estrogens. *Endocrinology* **131**, 655–661.
- (20) Ashburn, S. P., Han, X., and Liehr, J. G. (1993) Microsomal hydroxylation of 2- and 4-fluoroestradiol to catechol metabolites and their conversion to methyl esters: Catechol estrogens as possible mediators of hormonal carcinogenesis. *Mol. Pharmacol.* **43**, 534–541.
- (21) Bui, Q. D., and Weisz, J. (1988) Identification of microsomal, organic hydroperoxide-dependent catechol estrogen formation: Comparison with NADPH dependent mechanisms. *Pharmacology* **36**, 356–364.
- (22) Bunyagidj, C., and McLachlan, J. A. (1988) Catecholesterogen formation in mouse uterus. *J. Steroid Biochem.* **31**, 795–801.
- (23) Spink, D. C., Eugster, H. P., Lincoln, D. W., II, Schuetz, J. D., Schuetz, E. G., Johnson, J. A., Kaminsky, L. S., and Gierthy, J. F. (1992) 17 Beta-estradiol hydroxylation catalyzed by human cytochrome P450 1A1: A comparison of the activities induced by 2,3,7,8-tetrachlorodibenzo-p-dioxin in MCF-7 cells with those from heterologous expression of the cDNA. *Arch. Biochem. Biophys.* **293**, 342–348.
- (24) Liehr, J. G., Ricci, M. J., Jefcoate, C. R., Hannigan, E. V., Hokanson, J. A., and Zhu, B. T. (1995) 4-Hydroxylation of estradiol by human uterine myometrium and myoma microsomes: Implications for the mechanism of uterine tumorigenesis. *Proc. Natl. Acad. Sci. U.S.A.* **92**, 9220–9224.

³ Unpublished results (E. Cavalieri et al.).

- (25) Liehr, J. G., and Ricci, M. J. (1996) 4-Hydroxylation of estrogens as marker of human mammary tumors. *Proc. Natl. Acad. Sci. U.S.A.* **93**, 3294–3296.
- (26) NIH Guidelines for the Laboratory Use of Chemical Carcinogens (1981) NIH Publication No. 81-2385, U.S. Government Printing Office, Washington, DC.
- (27) Sanders, M., Hounk, K. N., Yun-Dong, W., Still, W. C., Lipton, M., Chang, G., and Guida, W. C. (1990) Conformations of cycloheptadecane. A comparison of methods for conformational searching. *J. Am. Chem. Soc.* **112**, 1419–1427.
- (28) Stewart, J. J. P. (1990) MOPAC: A semiempirical molecular orbital program. *J. Comput.-Aided Mol. Des.* **4**, 1–105.
- (29) Gross, M. L. (1990) Tandem mass spectrometry: Multisector magnetic instruments. In *Methods in Enzymology, Vol. 193, Mass Spectrometry* (McCloskey, J. A., Ed.) pp 131–153, Academic Press, San Diego.
- (30) Gross, M. L., Chess, E. K., Lyon, P. A., Crow, F. W., Evans, S., and Tudge, H. (1982) Triple analyzer mass spectrometry for high resolution MS/MS studies. *Int. J. Mass Spectrom. Ion Phys.* **42**, 243–254.
- (31) Abul-Hajj, Y. J., and Cisek, P. L. (1988) Catechol estrogen adducts. *J. Steroid Biochem.* **31**, 107–110.
- (32) Abul-Hajj, Y. J., Tabakovic, K., Gleason, W. B., and Ojala, W. H. (1996) Reactions of 3,4-estrone quinone with mimics of amino acid side chains. *Chem. Res. Toxicol.* **9**, 434–438.
- (33) Bolton, J. L., Acay, N. M., and Vukomanovic, V. (1994) Evidence that 4-allyl-*o*-quinones spontaneously rearrange to their more electrophilic quinone methides: Potential bioactivation mechanism for the hepatocarcinogen safrole. *Chem. Res. Toxicol.* **7**, 443–450.
- (34) Iverson, S. L., Hu, Q. L., Vukomanovic, V., and Bolton, J. L. (1995) The influence of *p*-alkyl substituent on the isomerization of *o*-quinones to *p*-quinone methides: Potential bioactivation mechanism for catechols. *Chem. Res. Toxicol.* **8**, 537–544.
- (35) Abul-Hajj, Y. J., Tabakovic, K., and Tabakovic, I. (1995) An estrogen–nucleic acid adduct. Electroreductive intermolecular coupling of 3,4-estrone-*o*-quinone and adenine. *J. Am. Chem. Soc.* **117**, 6144–6145.
- (36) RamaKrishna, N. V. S., Cavalieri, E. L., Rogan, E. G., Dolnikowski, G. G., Cerny, R. L., Gross, M. L., Jeong, H., Jankowiak, R., and Small, G. J. (1992) Synthesis and structure determination of the adducts of the potent carcinogen 7,12-dimethylbenz[*a*]anthracene and deoxyribonucleosides formed by electrochemical oxidation: Models for metabolic activation by one-electron oxidation. *J. Am. Chem. Soc.* **114**, 1863–1874.
- (37) Rogan, E., Cavalieri, E., Tibbels, S., Cremonesi, P., Warner, C., Nagel, D., Tomer, K., Cerny, R., and Gross, M. (1988) Synthesis and identification of benzo[*a*]pyrene–guanine nucleoside adducts formed by electrochemical oxidation and horseradish peroxidase-catalyzed reaction of benzo[*a*]pyrene with DNA. *J. Am. Chem. Soc.* **110**, 4023–4029.
- (38) RamaKrishna, N. V. S., Gao, F., Padmavathi, N. S., Cavalieri, E. L., Rogan, E. G., Cerny, R. L., and Gross, M. L. (1992) Model adducts of benzo[*a*]pyrene and nucleosides formed from its radical cation and diol epoxide. *Chem. Res. Toxicol.* **5**, 293–302.
- (39) Tomer, K. B., and Gross, M. L. (1988) Fast atom bombardment and tandem mass spectrometry for structure determination: Remote site fragmentation of steroid conjugates and bile salts. *Biomed. Environ. Mass Spectrom.* **15**, 89–98.
- (40) Chakravarti, D., Pelling, J. C., Cavalieri, E. L., and Rogan, E. G. (1995) Relating aromatic hydrocarbon-induced DNA adducts and *c*-Harvey-*ras* mutations in mouse skin papillomas: The role of apurinic sites. *Proc. Natl. Acad. Sci. U.S.A.* **92**, 10422–10426.

TX960002Q